Available online at www.eccomasproceedia.org
Eccomas Proceedia COMPDYN (2017) 4675-4690

ECCOMAS
Proceedia

COMPDYN 2017
6th ECCOMAS Thematic Conference on
Computational Methods in Structural Dynamics and Earthquake Engineering
M. Papadrakakis, M. Fragiadakis (eds.)
Rhodes Island, Greece, 15–17 June 2017

STATIC AND DYNAMIC BEHAVIOUR OF PILE FOUNDATIONS IN HOMOGENEOUS AND INHOMOGENEOUS SOILS

Lutz Auersch[1], **Greta Markfort**[1]

[1] Federal Institute of Materials Research and Testing (BAM),
D 12200 Berlin, Germany
e-mail: lutz.auersch-saworski@bam.de

Keywords: pile foundation, finite-element boundary-element method, pile bending stiffness, soil stiffness, continuously inhomogeneous soils, layered soils, wind energy tower.

Abstract. *Offshore wind energy towers are dynamically loaded by waves and wind. Pile foundations provide stiffness and damping and should be properly calculated. A combined finite-element boundary-element method for the dynamic interaction of flexible structures and the soil has been developed. The flexible structures such as single piles or complete wind energy towers are modeled by the finite element method whereas the homogeneous or layered soil is modeled by the boundary element method which uses the Green's functions for interior loads in the layered half-space to establish the dynamic stiffness matrix of the soil. Soils with a stiffness that is continuously increasing with depth can be modeled as multi-layer soils with step-wise increasing stiffness. The effects of different parameters such as the stiffness of the soil, the axial and bending stiffness of the pile, and the radius of the cylindrical contact area will be analysed for the different components of excitation (vertical, horizontal, rotation and coupling). The results can be determined as specific power laws which are different for the different load cases and for the different soil models (Winkler support, homogeneous continuum, continuum with increasing stiffness). The dynamic effect of radiation damping will be analysed by the frequency-dependent compliance functions. A clear layering of the soil can cause noticeable changes in the dynamic compliances as reductions of the stiffness and the damping in certain frequency ranges (below and around layer resonance frequencies). The distribution of the displacements along the pile help to explain the observed laws. An example of an offshore wind energy tower has been modeled and calculated for wind, wave and weight loads. The resonances of the tower are usually limited by the radiation damping which is strongest for a soft soil.*

Peer-review under responsibility of the organizing committee of COMPDYN 2017.
doi: 10.7712/120117.5753.17389

1 INTRODUCTION

The problem of the foundation of wind energy towers is outlined in Figure 1. The high (offshore) wind energy towers are founded on thick monopiles or on jackets which stand on four thinner piles. This contribution presents a method to calculate the dynamics of piles in a continuum soil (section 2), performs a parametric study for a single jacket pile in a homogeneous soil (section 4) or different inhomogeneous soils (section 5) and demonstrates the consequences for a wind energy tower on a monopile (section 6).

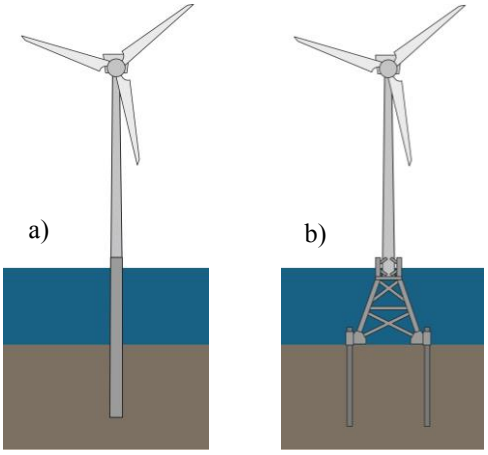

Figure 1: Offshore wind energy towers with a) monopile foundation and b) jacket-pile foundation.

2 COMBINED FINITE-ELEMENT BOUNDARY-ELEMENT METHOD

The dynamic soil-structure interaction is analysed by a combined finite-element boundary-element method [1]. Flexible structures such as beams, plates, walls, box-type buildings, railway tracks, single piles and pile groups are modeled by the finite element method whereas the homogeneous or layered soil is modeled by the boundary element method. A point load, a wheel-set load or and a wave field have been used as excitation. In this contribution, single piles and wind energy towers are presented.

The basis is the point-load solution (Green's function) for a layered soil. The Green's functions are calculated by the following procedure. For each layer, a 4x4 symmetric stiffness matrix is calculated in wave number domain [2]. All layer matrices and the matrix of the underlying half-space are assembled in a stiffness matrix $\mathbf{K}_S$ of the whole soil body, which is inverted to a compliance matrix $\mathbf{N}$. The appropriate elements of this compliance matrix, for example $N_{zz}(k,z_1,z_2)$ for an interior source at z_1 and an interior response at z_2, are integrated over the wave number k to get the displacement at a distance r of the source

$$F_{zz}(r,z_1,z_2) = \frac{1}{2\pi}\int_0^\infty N_{zz}(k,z_1,z_2)\mathrm{J}_0(kr)kdk \tag{1}$$

Similar formulas hold for the other four components of the Green's function F. These Green's functions are used in the combined finite-element boundary-element method to establish a boundary stiffness matrix of the soil (in frequency domain, for n discrete points). A displacement matrix is compiled directly by using the point-load solutions

$$\mathbf{u}(\mathbf{x}_\beta) = \mathbf{F}(\mathbf{x}_\beta\text{-}\mathbf{x}_\alpha)\,\mathbf{p}(\mathbf{x}_\alpha) \qquad \mathbf{u}_\beta = \mathbf{F}_{\beta\alpha}\,\mathbf{p}_\alpha \tag{2}$$

At the loading point, this would yield infinite values. Therefore, mean values on the cylindrical (in case of a pile) or circular surface (in case of a surface foundation) are calculated as the diagonal elements of the displacement matrix

$$\mathbf{u}_\alpha = \frac{1}{A_\alpha}\int_{A_\alpha}\mathbf{F}(\mathbf{x}-\mathbf{x}_\alpha)\mathbf{p}(\mathbf{x}_\alpha)\,dA \qquad \mathbf{u}_\alpha = \mathbf{F}_{\alpha\alpha}\,\mathbf{p}_\alpha \tag{3}$$

The force matrix of the soil is the identity matrix, as 1) the Green's function has no stresses at the soil surface and 2) the stresses in the interior do not yield forces at another pile element (as far as the dimension is small compared to the distance and wavelength). Thus, the inverse of the displacement matrix $\mathbf{U} = [\mathbf{F}_{\alpha\beta}]_{\alpha,\beta=1,n}$ is the boundary stiffness matrix $\mathbf{K}_S$ of the soil

which is added to the finite-element stiffness matrix $\mathbf{K}_P$ of the structure to yield the global dynamic stiffness matrix $\mathbf{K}_S+\mathbf{K}_P$ of the combined structure-soil system, and the FEBE method is complete.

3 PILE AND SOIL PARAMETERS AND THEIR VARIATION

A typical tubular steel pile of a jacket foundation of an offshore wind energy tower is analysed with the following standard parameters [3]: The mass density $\rho_P = 7.8\ 10^3$ kg/m^3, and the elasticity modulus $E_P = 2.1\ 10^{11}$ N/m^2 of steel, a circular cross section of radius $R = 1$ m, a wall thickness of $t = 0.03$ m, yielding a longitudinal stiffness of $EA = 0.4\ 10^{11}$ N, a bending stiffness of $EI = 1.9\ 10^{10}$ Nm^2, and a mass per length $m' = 1.48\ 10^3$ kg/m. The length of the pile is $L = 30$ m, the material damping is defined as $D_P = 0$.

The standard soil is homogeneous with the following parameters: The shear modulus is $G = 8\ 10^7$ N/m^2, the mass density $\rho = 2\ 10^3$ kg/m^3, the material damping $D = 2.5\%$, and the Poisson's ratio $\nu = 0.33$, which yield the shear wave velocity $v_S = 200$ m/s, and the compressional wave velocity $v_P = 400$ m/s.

The stiffness of the homogeneous soil is varied as $G = 2, 4.5, 8, 18\ 10^7$ N/m^2. Three other soil models are analysed: layered soils and two soils with a continuous variation. The continuous variations are defined as a function of z

$G(z) = G'z$ linear variation and

$G(z) = G^*\sqrt{z}$ parabolic variation.

The new soil parameters are varied as $G' = 2, 4.5, 8, 18\ 10^7$ N/m^3, and $G^* = 2, 4.5, 8, 18\ 10^7$ N/m$^{2.5}$. By this definition all soil models have the same stiffness at 1 m depth. The layered soil has a soft top layer of $G_1 = 2\ 10^7$ N/m^2 and a stiff underlying half-space of $G_2 = 5\ 10^8$ N/m^2, and the layer height is varied as $H = 2.5, 5, 10, 20, 30$ m.

The results are presented as four frequency-dependent complex compliance functions for the horizontal, the vertical, the rocking and the horizontal-rocking coupling mode. The static deformations of all pile foundations are given in the appendix for a better interpretation.

4 COMPLIANCE FUNCTIONS OF PILES IN HOMOGENEOUS SOILS

The compliance functions of the pile foundations are presented as amplitude and phase in the frequency range between 0 to 16 Hz. The principle behavior can be discussed with the horizontal component in Figure 2a. The amplitudes show only little variations with frequency, whereas the phase is continuously decreasing with frequency. The horizontal component has the most regular phase behavior, the phase delay increases almost linearly with frequency.

The corresponding horizontal deformation is shown in the Appendix, Fig. 8a. The displacement has its maximum at the top of the pile. The displacements decrease rapidly with the depth and reaches almost zero at 10 m. Therefore, it can be concluded that the standard pile of 30 m length behaves like an infinitely long pile for the horizontal vibration modes.

The vertical vibration component is completely different (Fig. 8b). The vertical displacements change only a little along the pile length of 30 m. At the pile end, there are still considerable amplitudes, and that means that the pile behaves like an almost rigid pile in the vertical direction. The rocking and coupling components display at least one change of sign before the displacements vanish at 15 or 20 m depth. The decrease is as strong as for the horizontal component, the first minimum can be found at 5 to 7 m depth.

The rocking and coupling compliances in Figure 2c and 2d can therefore be read as the compliances of infinitely long piles. They have also nearly constant amplitudes and decreasing phases. The phase delay has one difference compared to the horizontal one. It starts not at zero frequency but at a later frequency of 4 to 8 Hz (rocking) or 2 to 4 Hz (coupling). The

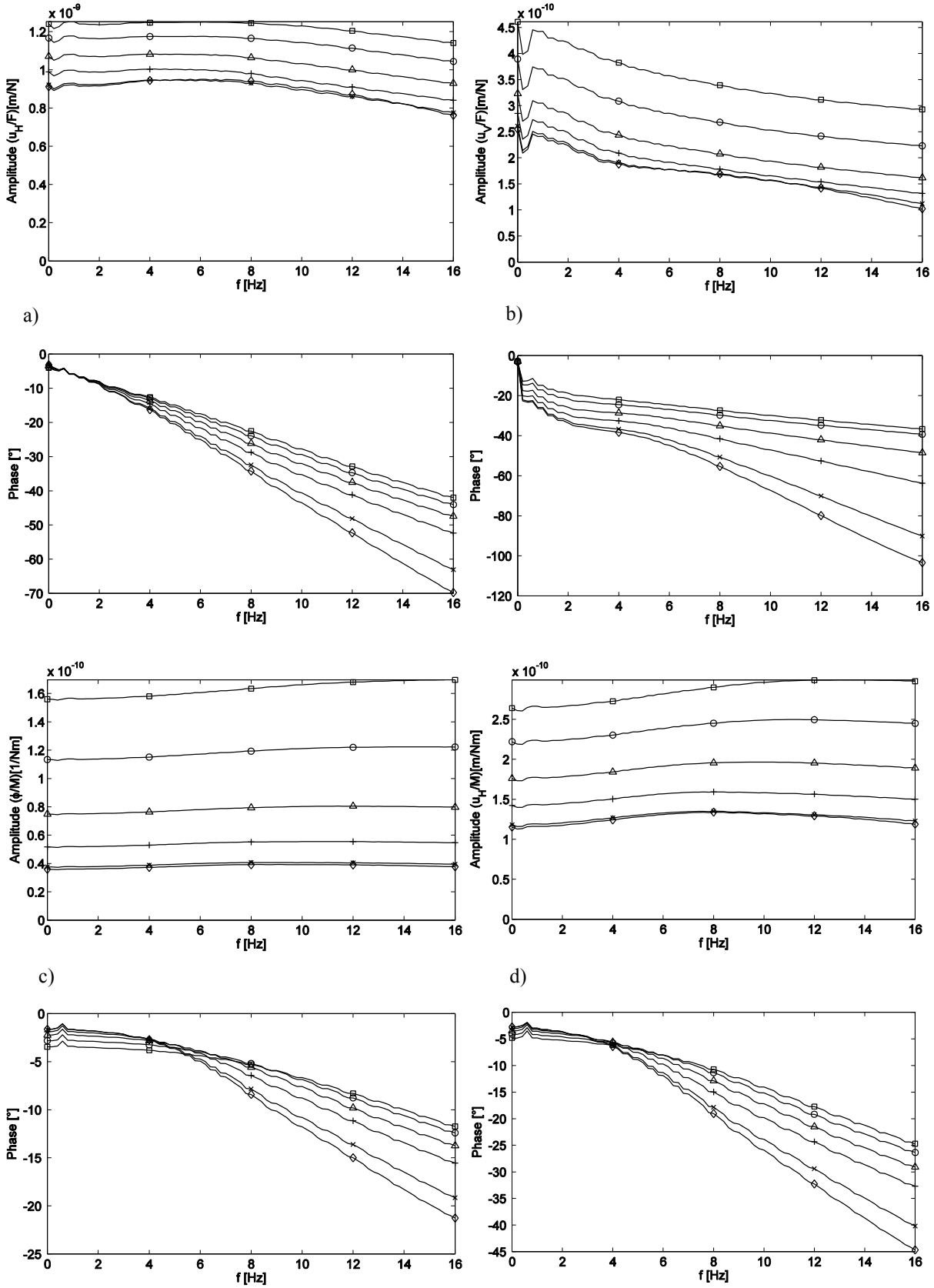

Figure 2: Amplitude and phase of the a) horizontal, b) vertical, c) rocking, and d) coupling compliance of the standard pile foundation. Variation of the wall thickness t = □ 0.03, ○0.05, △ 0.1, + 0.2, ×0.5, ◇ 1 m.

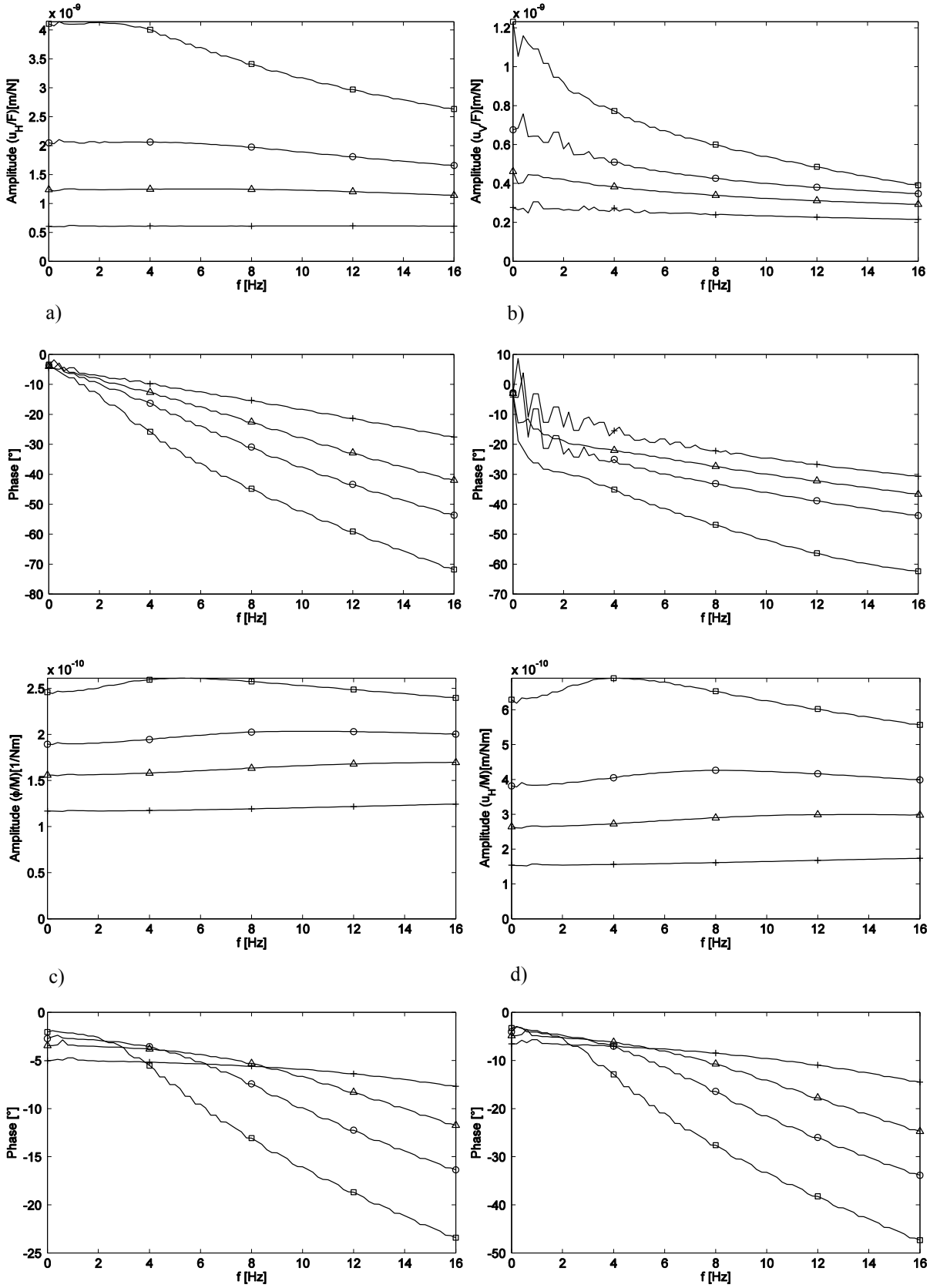

Figure 3: Amplitude and phase of the a) horizontal, b) vertical, c) rocking, and d) coupling compliance of the standard pile foundation. Variation of the soil stiffness G = □ 2, ○ 4.5, △ 8, + 18 10^7 N/m^2.

maximum phase delay at 16 Hz is only 12 to 22° for the rocking and 25 to 45° for the coupling component. This is small compared to 41 to 70° for the horizontal component. This sequence horizontal, coupling, rocking will be found also for other characteristics.

The influence of the pile bending stiffness on the compliances is strongest for the rocking, mid-strong for the coupling, and weakest for the horizontal component. The highest factor between the softest and the stiffest pile is $A_1/A_2 = 1.6/0.4 = 4$ (rocking), the lowest factor is $A_1/A_2 = 1.25/0.9 = 1.4$ (horizontal), whereas the ratio of the bending stiffness is $EI_2/EI_1 = 0.79/0.09 = 8.8$.

While Figure 2 shows the influence of the pile bending stiffness, Figure 3 demonstrates the influence of the soil stiffness which is varied in the range of $G_2/G_1 = 18/2 = 9$. The horizontal response varies quite strong between 0.6 and 4.1 10^{-9} m/N, a factor of 7 close to the variation of the soil stiffness. Quite contrary, the rocking amplitude displays the weakest influence of the soil stiffness. The phases of the compliance, which correlate well with the damping of the pile foundation, are strongly influenced by the soil stiffness for all components. The maximum phase delay at 16 Hz is 28 to 71° (horizontal), 14 to 48° (coupling) and 7.5 to 23° (rocking). (This is approximately $\varphi \sim G^{-0.5}$, whereas the influence of the pile stiffness is only $\varphi \sim EI^{-0.25}$.) The damping by the radiation into the soil starts at higher frequencies for the stiffer soils, at about 12 Hz for the rocking and at about 8 Hz for the coupling component. The damping of the horizontal component starts at zero frequency.

When looking at the deformations in Fig. 9, the influence of the soil is clearly stronger than the influence of the pile (Fig. 8) although the variations of $G_2/G_1 \approx EI_2/EI_1 \approx 9$ are almost the same. A soft soil yields a much deeper horizontal deformation (up to $z = 15$ m) than a stiff soil ($z = 5$ m).

5 THE PILES IN INHOMOGENEOUS SOILS

5.1 Soil with parabolic increase of stiffness with depth (“parabolic soil”)

A soil body is loaded by its own weight. The static pressure is linearly increasing with depth and yields a stiffening of the soil. The influence of the static pre-stress is in that way that the stiffness of the soil increases with the square root of the depth. This natural soil model has the smoothest variation of G and is presented in Figure 4 (compliance functions) and Figures 10 (deformation).

The deformation of the “parabolic soil” (Fig. 10) is more restricted to the near-surface soil compared to the homogeneous half-space (Fig. 9). This holds for all compliance components. The amplitudes of the compliances seem to follow the same rules as for the homogeneous soil: The influence of the soil is increasing in the order rocking, coupling, and horizontal component. The main difference to the homogeneous soil can be found for the phase functions (the damping). The damping values are considerably reduced, see Table 1. The starting point of the radiation damping is shifted to higher frequencies, for example from 2 to 4 Hz for the softest soil and the rocking component (Figs. 3c and 4c). Moreover, the damping of the horizontal component does no longer start at zero frequency, but has its own starting frequency between 2 and 5 Hz (Fig. 4a).

5.2 Soil with linear increase of stiffness with depth (“linear soil”)

The soil model with a linearly increasing stiffness is a more theoretical model which has a stronger variation $G(z)$. The shear modulus at 1 m depth is the same for the homogeneous, the parabolic and the linear soil model. The stiffness of shallower depths is lowest for the linear and highest for the homogeneous soil model, and the stiffness at greater depths is highest for

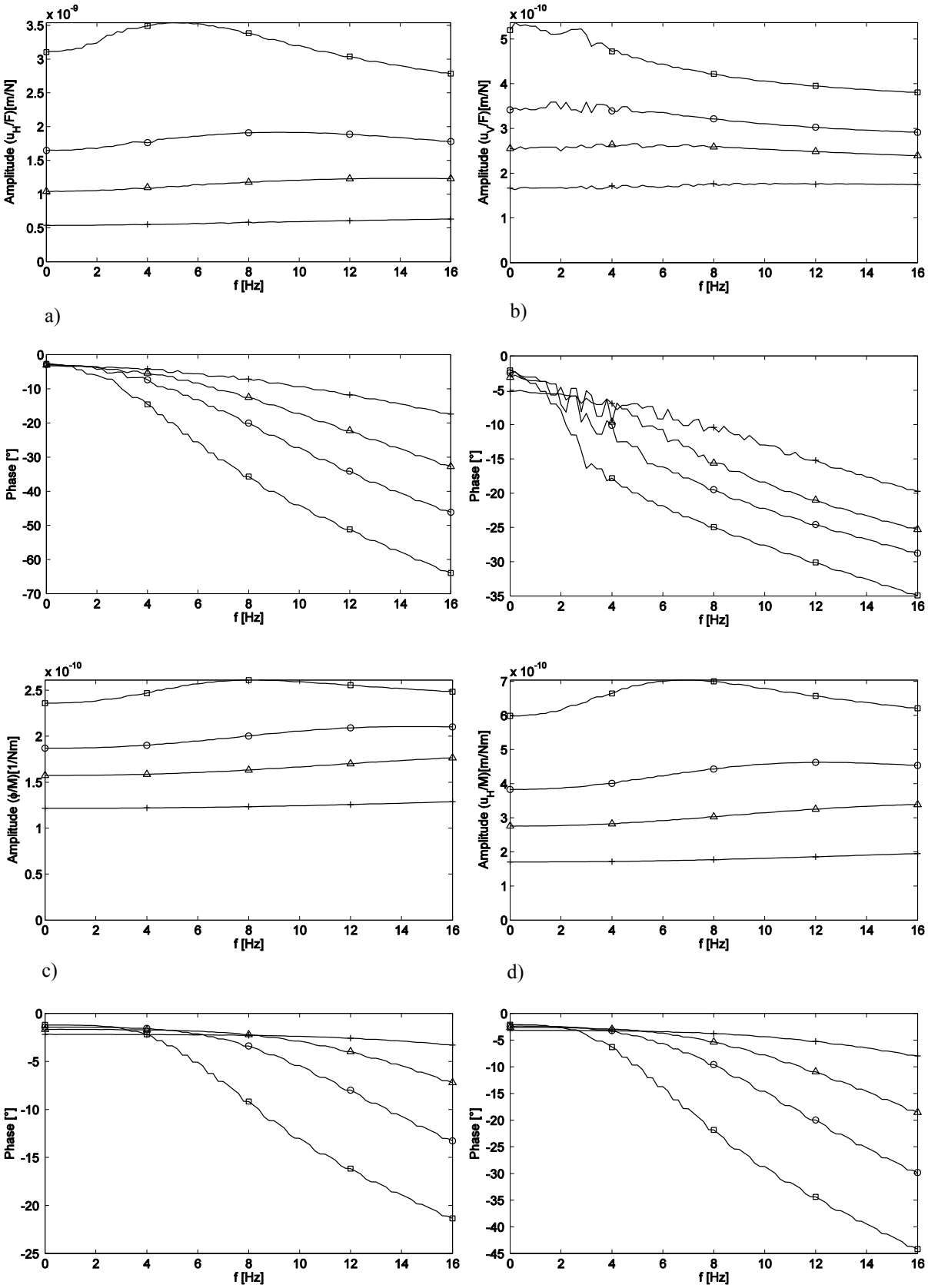

Figure 4: Amplitude and phase of the a) horizontal, b) vertical, c) rocking, and c) coupling compliance of the standard pile in parabolic soil. Variation of the soil stiffness G^* = □ 2, ○ 4.5, △ 8, + 18 10^7 N/m$^{2.5}$.

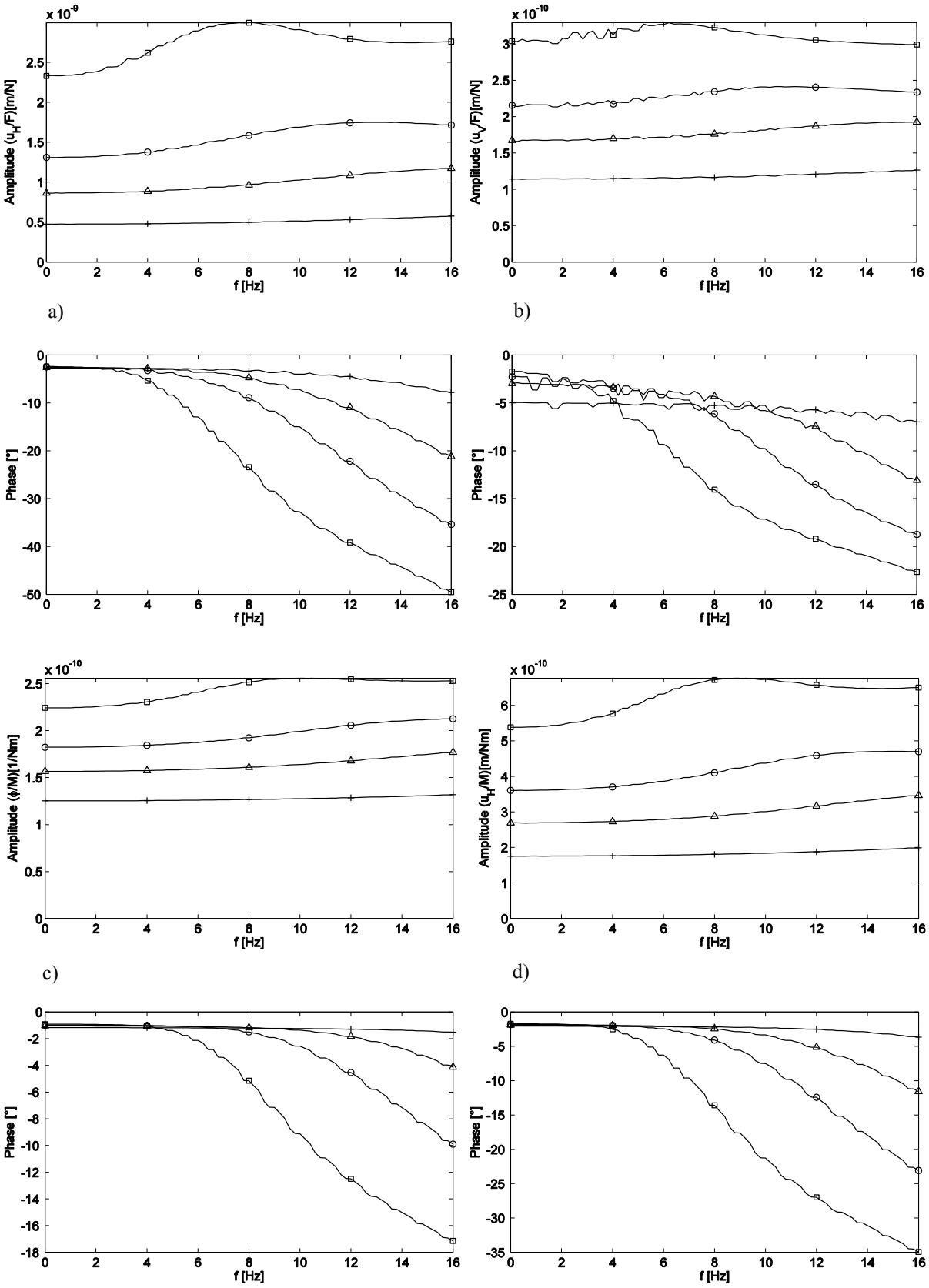

Figure 5: Amplitude and phase of the a) horizontal, b) vertical, c) rocking, and c) coupling compliance of the standard pile in linearly varying soil. Variation of the soil stiffness G' = □ 2, ○ 4.5, △ 8, + 18 10^7 N/m^3.

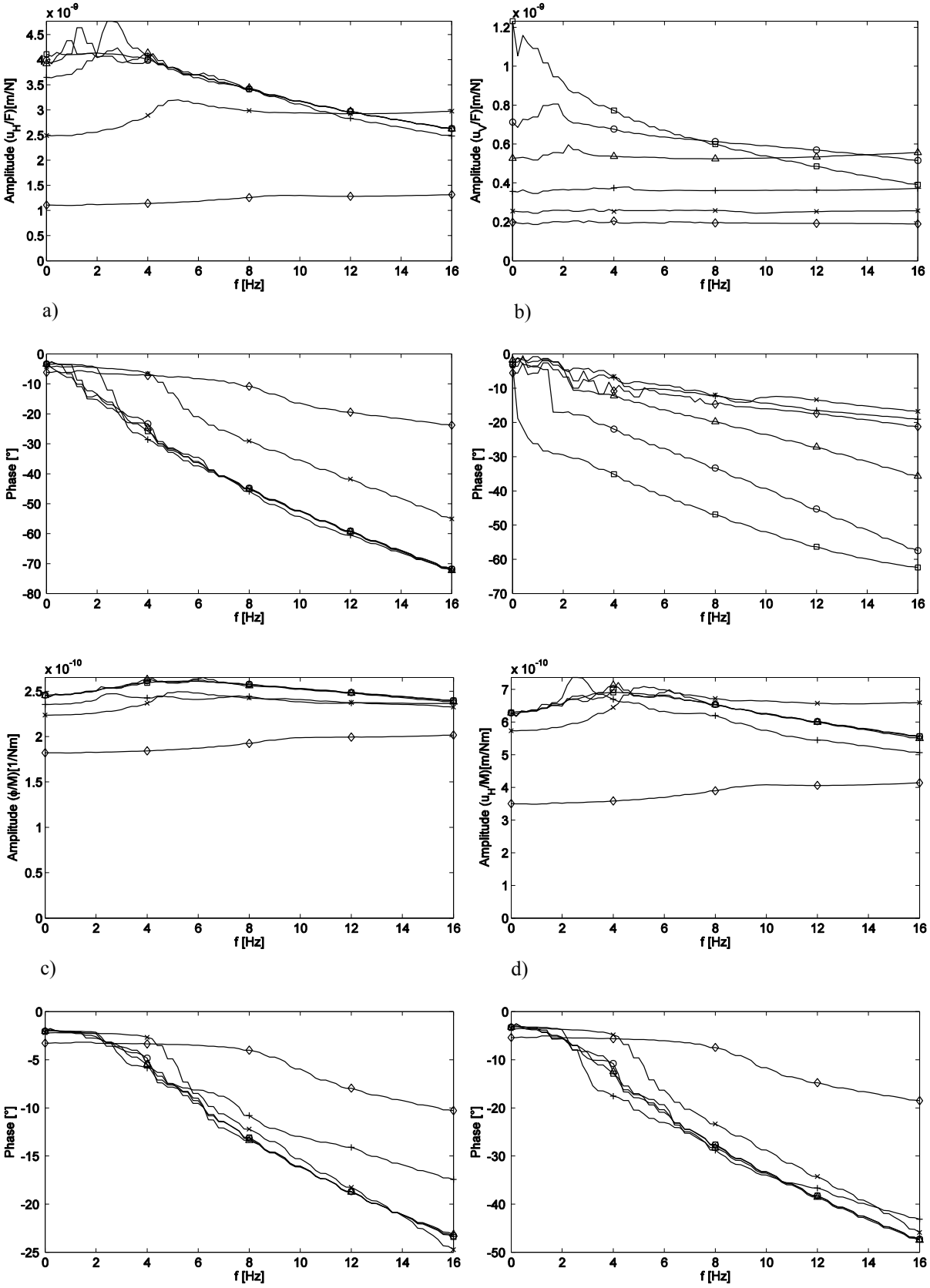

Figure 6: Amplitude and phase of the a) horizontal, b) vertical, c) rocking, and c) coupling compliance of the pile in layered soils (G_1/G_2 = 2/50), variation of the layer height H = □ ∞, ○ 30, △ 20, ＋10, × 5, ◇ 2.5 m.

the linear and lowest for the homogeneous soil. The linear soil model shows the same characteristics as the parabolic soil, but all in a stronger realization. The deformation is concentrated on shallower depths (Fig. 11), the damping (the phase delay) starts at higher frequencies and reaches lower maximum values, see Figure 5 and Table 1.

variation	Figure	horizontal	coupling	rocking
pile stiffness	2	40°-70°	25°-45°	12°-22°
homogeneous soil	3	28°-71°	14°-48°	7.5°-24°
parabolic soil	4	18°-63°	8°-45°	3°-22°
linear soil	5	8°-50°	3°-35°	1.5°-17°
layered soil	6	22°-72°	18°-48°	10°-23°

Table 1: Damping expressed as the phase delay of the different compliance components for the parameter variations in Figures 2 to 6.

5.3 Layered soils with different layer heights

The layered soils have some similarities to the continuously varying soil models, but also some additional characteristics. Similarly, the displacements approach faster the zero (Fig. 12 compared to Fig. 9). Similarly, the phase delays are smaller (Fig. 6). In addition, small peaks can be found in the compliances, for example at $f = 0.7$, 1.3, 2.6, 4.8, 8.5 Hz for the horizontal component (Fig. 6a). At the same frequencies, the phase delay (the radiation damping) starts. These frequencies are the resonant frequencies of the layer $f_L = v_S/4H$ (= 0.8, 1.25, 2.5, 5, 10 Hz). Deep layers have a low layer frequency so that only the low frequencies are concerned. On the other hand, the shallow layers affect a wider frequency range, but it should be stated that the damping is not zero below the layer frequency. The low frequency damping follows the damping of the stiff underlying half-space. Another special point is that a layering deeper than 10 m has little effect on the results. The results are almost the same as for the soft half-space (curve □ in Fig. 6) because the deformation for a soft half-space does not reach beyond 10 m (Fig. 9). In case of shallow layers, the compliances are reduced by the stiff underlying half-space, most strongly for the horizontal component where $A_L/A_H = 1/4$ for $H = 2.5$ m and $A_L/A_H = 2.5/4 = 0.6$ for $H = 5$ m.

6 EVALUATION OF STATIC RULES

The influence of the bending stiffness EI of the pile and the stiffness G of the soil on the compliances of the pile foundation can be analysed in more detail. It is convenient to use the ratio of the pile and soil stiffness as the elastic length

$$l = \sqrt[4]{\frac{EI}{G}} \quad . \tag{4}$$

The static compliances of an infinitely long pile can then be presented as

$$\frac{u}{F} = \frac{1}{Gl} f_1\left(\frac{R}{l}\right) \qquad \frac{u}{M} = \frac{1}{Gl^2} f_2\left(\frac{R}{l}\right) \qquad \frac{\varphi}{M} = \frac{1}{Gl^3} f_3\left(\frac{R}{l}\right) \tag{5}$$

with the n-th power (n = 1, 2, 3) of the elastic length. The numerical results of section 4 (homogeneous soils) are evaluated for the functions $f_i(R/l)$ which are power functions with the power q

$$\frac{u}{F} \sim \frac{1}{Gl}\left(\frac{R}{l}\right)^{-q} \quad \text{or} \quad \frac{F}{u} \sim Gl\left(\frac{R}{l}\right)^{q} = R^q EI^{\frac{1}{4}-\frac{q}{4}} G^{\frac{3}{4}-\frac{q}{4}} = R^q EI^{0.13} G^{0.87} \tag{6}$$

with the power $q = 0.49$ for the horizontal compliance in a homogeneous soil. The equation expresses the strong influence of the soil on the horizontal compliance and, at the same time, the weak influence of the pile. The exponents of the power laws for all compliance or stiffness components are compiled in Table 2.

In case of the continuously inhomogeneous soils, the stiffness of the soil is expressed by different moduli which yield different elastic lengths

$$G^* = \frac{G}{\sqrt{z}} \quad \text{and} \quad l^* = \sqrt[4.5]{\frac{EI}{G^*}} \qquad\qquad G' = \frac{G}{z} \quad \text{and} \quad l' = \sqrt[5]{\frac{EI}{G'}} \tag{7}$$

where the fourth root is replaced by a higher root with 4+p, p = 0.5 or 1.0. Finally, the stiffnesses of different components and different soil models can be calculated as

$$K \sim R^q EI^{\frac{n+p-q}{4+p}} G^{1-\frac{n+p-q}{4+p}} \tag{8}$$

The exponents of all power laws follow from the corresponding exponent *q,* which has been derived from the FEBEM calculations, and are given in Table 2.

parameter	component	homogeneous	parabolic	linear
radius R	horizontal	0.49	0.59	0.62
	coupling	0.57	0.58	0.56
	rocking	0.36	0.33	0.36
pile stiffnesss EI	horizontal	0.13	0.20	0.28
	coupling	0.36	0.43	0.49
	rocking	0.66	0.70	0.73
soil stiffness G, G*, G’	horizontal	0.87	0.80	0.72
	coupling	0.64	0.57	0.51
	rocking	0.34	0.30	0.27

Table 2: Exponents of the power laws for the static stiffnesses of pile foundations

The strong influence of the soil for horizontal excitation can be found for all soil models as well as the reduced soil influence for the coupling and especially for the rocking excitation. The more inhomogeneous the soil is, the weaker is its influence on the foundation stiffness components. While a homogenous soil has a much stronger influence than a Winkler support, the linearly inhomogeneous soil has nearly the lower powers of the Winkler soil (0.75, 0.5 0.25 for the influence of the homogeneous bedding modulus on the horizontal, coupling and rocking component). The influence of the pile radius as parameter of the pile-soil contact has been found similarly strong for the three continuous soil models.

7 WIND ENERGY TOWER

An offshore wind energy tower of total length $L = L_T+L_W+L_P$ = 70+20+30 m = 120 m has been modelled in detail. The tower is founded on a monopile foundation with a pile radius of R = 3 m and a wall thickness of t = 0.06 m. The tower has a thinner wall above the water level where the thickness is in the range of t = 0.034 to 0.016 m decreasing with height. The tower

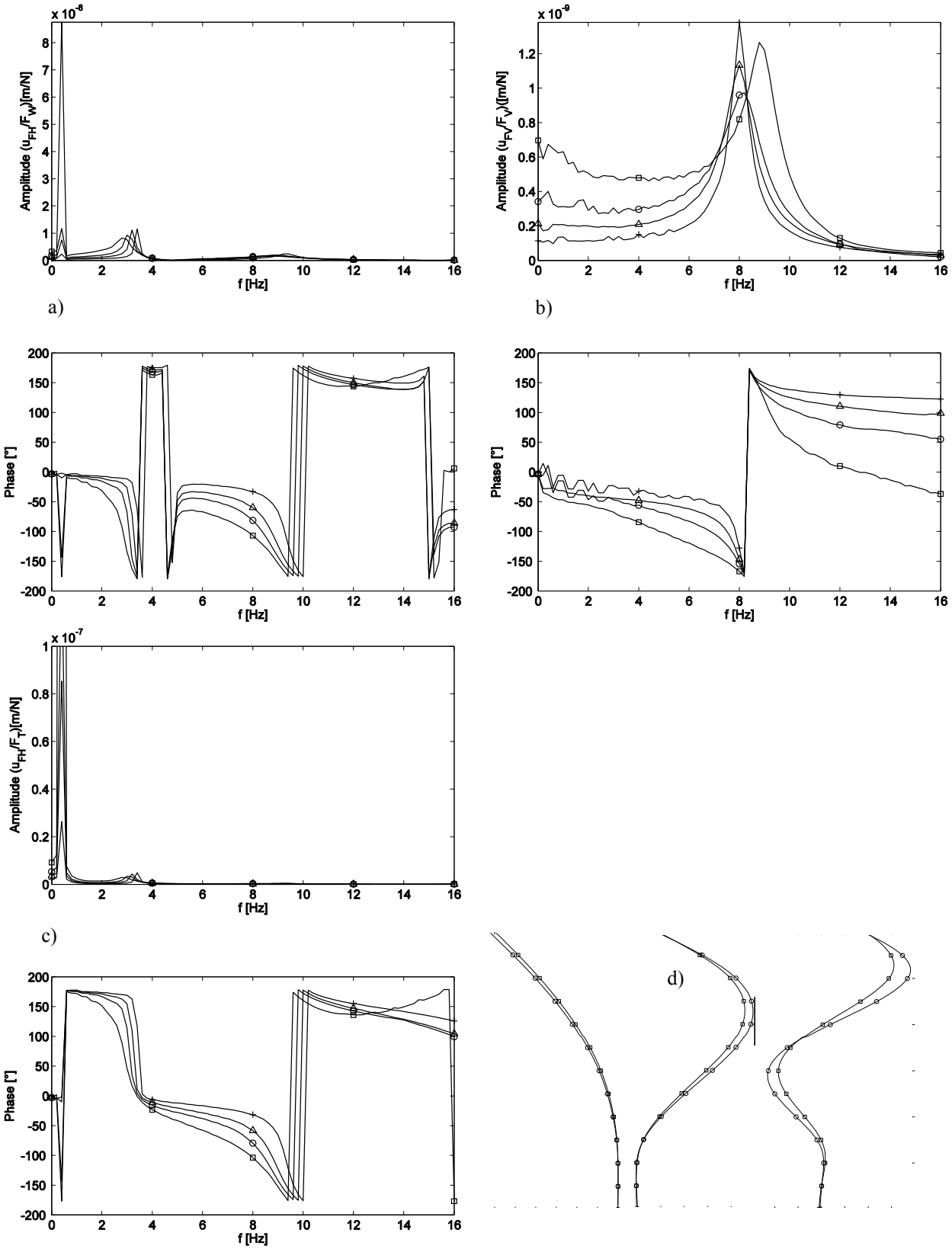

Figure 7: Amplitude and phase of the transfer functions of a wind energy tower, a) horizontal wave load, b) vertical top load, c) horizontal wind load, response at the top of the pile, variation of the soil stiffness G = □ 2, ○ 4.5, △ 8, + 18 10^7 N/m^2. d) 1st, 2nd, 3rd horizontal mode

radius becomes smaller with increasing height from $R = 3$ m to 2 m on the top 35 meters. On the top of the tower, a concentrated mass of 300.000 kg is assumed to represent the rotor and the nacelle. The wind energy tower is excited by horizontal wind loads F_T at the top of the tower, by horizontal wave loads F_W at the sea level, and by vertical loads F_V at the top of the tower (machine loads, weight). The corresponding horizontal and vertical responses are analysed at the top of the pile foundation.

Figure 7 shows the transfer functions of the pile foundations for all three excitations and for four different homogeneous soils. The vertical load yields a vertical resonance at 8 Hz (Fig. 7b). The horizontal loads yield three resonances up to 16 Hz (Fig. 7a,c). The vibration modes at 0.4, 3.6, and 8.4 Hz in Figure 7d can be characterized as 1) a dominant tower top motion, 2) a dominant mid-tower vibration with one maximum, and 3) a tower vibration with two opposite maxima. The heavy top mass has reduced amplitudes for the 3rd and especially for the 2nd vibration mode.

The 2nd and 3rd horizontal resonance frequencies are increased with a stiffer soil. The resonance amplitudes also increase with increasing soil stiffness. Thus, a soft soil is advantageous because of its higher radiation damping. On the other hand, the soft soil causes a higher static response which can yield a higher resonance amplitude as in Figure 7b. If the material damping is dominant over the small radiation damping at very low frequencies, the order of the amplitudes can be even reverse (Fig. 7a). Obviously, the correct behavior of the pile foundation is important for the response of wind energy towers to dynamic loads.

8 CONCLUSION

The soil has a strong influence on the dynamic compliance, the stiffness and damping, of pile foundations. This influence has been quantified for homogeneous, continuously inhomogeneous, and layered soil models. The influence of the soil increases from the rocking to the coupling to the horizontal foundation stiffness. The influence also increases from the most inhomogeneous soil with linearly increasing modulus to the less inhomogeneous parabolic soil to the homogeneous soil. The same rules hold for the damping which is strongest for a homogeneous soil and the horizontal component. The damping of all inhomogeneous soils and the damping of the rocking and coupling component have almost zero damping at low frequencies. The results for the dynamic pile compliances are used to calculate the response of an example wind energy tower demonstrating the damping effects of different homogeneous soils.

ACKNOWLEDGEMENT

G. Markfort has performed the calculations and evaluations at BAM as her bachelor thesis for the University of Applied Sciences Kiel, Prof. C. Keindorf. L. Auersch has developed the FEBEM-software, has been the adviser, and has written the article.

REFERENCES

[1] L. Auersch, *Wechselwirkung starrer und flexibler Strukturen mit dem Baugrund insbesondere bei Anregung durch Bodenerschütterungen*. BAM-Research Report 151/Thesis, Berlin, 1988.

[2] L. Auersch, Wave propagation in the elastic half-space due to an interior load and its application to ground vibration problems and buildings on pile foundations. *Soil Dynamics and Earthquake Engineering* **30**, 925-936, 2010.

[3] G. Markfort, *Dynamische Steifigkeiten in Abhängigkeit von Boden- und Pfahlparametern bei Tiefgründungen von Offshore-Windenergieanlagen*. Bachelor Thesis, University of Applied Sciences, Kiel, 2017.

APPENDIX: PILE DEFORMATIONS

The following Figures 8 to 12 present the static deformations of all pile foundations of the parameter variation. Sub-figures a show the horizontal displacements due to the horizontal load which are usually smoothly approaching zero. The vertical displacements due to the vertical load in sub-figures b have only a weak reduction along the pile length. The response to a moment is given in sub-figures c and d (the rotation and the displacement) which both show one or more changes of sign before they approach zero. The approach to zero is faster for stiffer and for more inhomogeneous soils. A softer soil or a stiffer pile yield a deeper deformation or in other words a longer elastic length means a longer or deeper deformation.

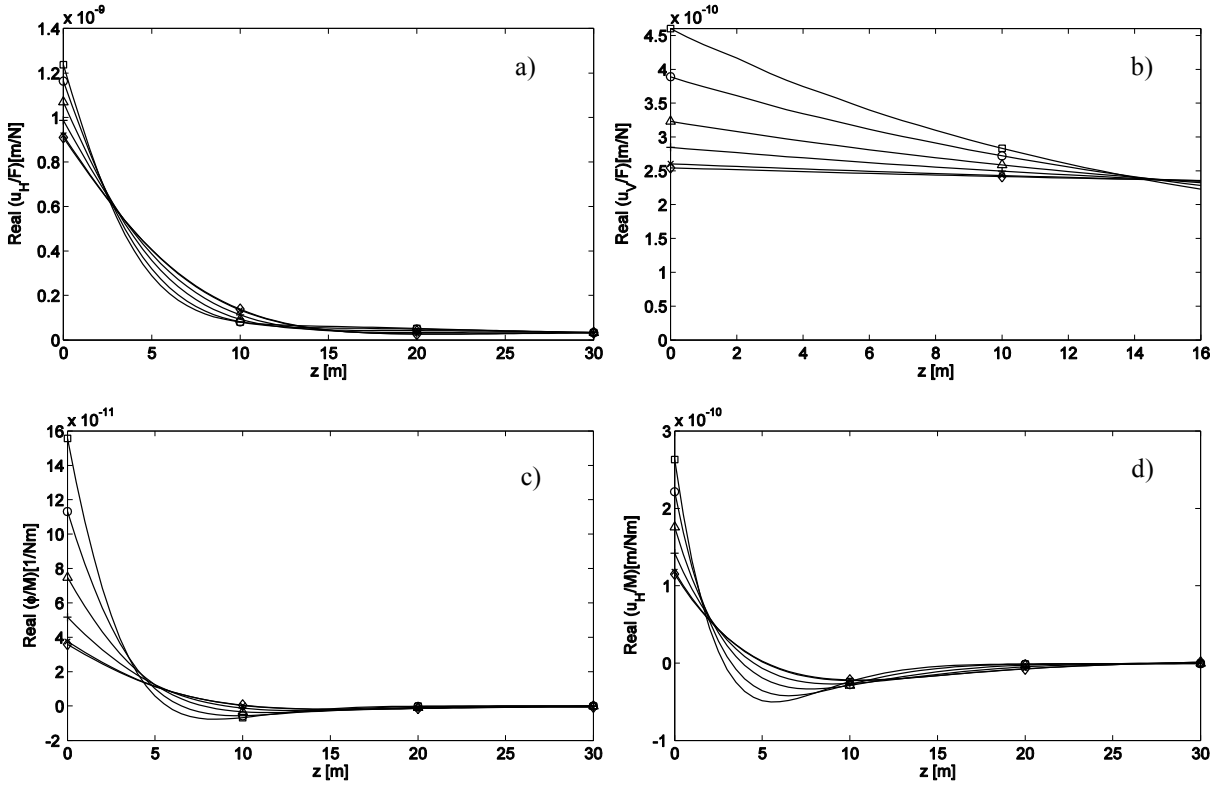

Figure 8: Static deformation of the standard pile foundation, the a) horizontal, b) vertical, c) rocking, and d) coupling component. Variation of the wall thickness t = □ 0.03, ○ 0.05, △ 0.1, + 0.2, × 0.5, ◇ 1 m.

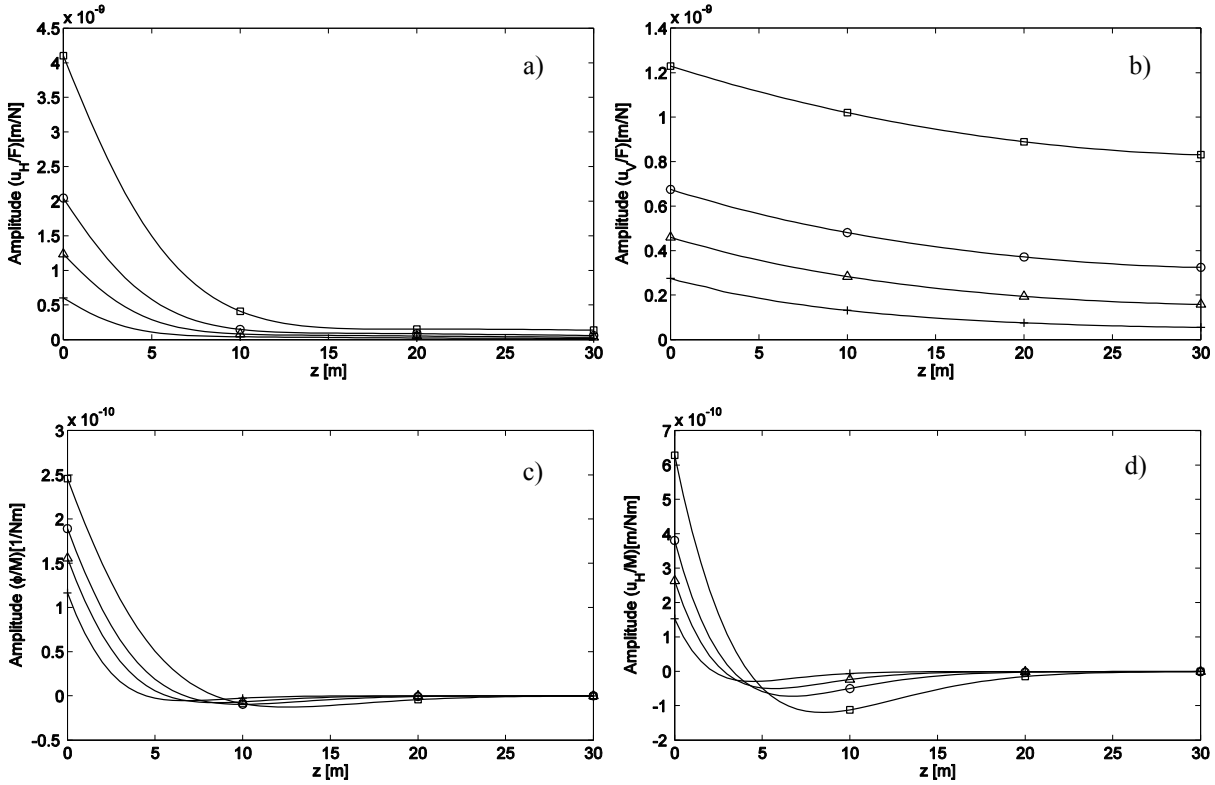

Figure 9: Static deformation of the standard pile foundation, the a) horizontal, b) vertical, c) rocking, and d) coupling component. Variation of the soil stiffness G = □ 2, ○ 4.5, △ 8, + 18 10^7 N/m^2.

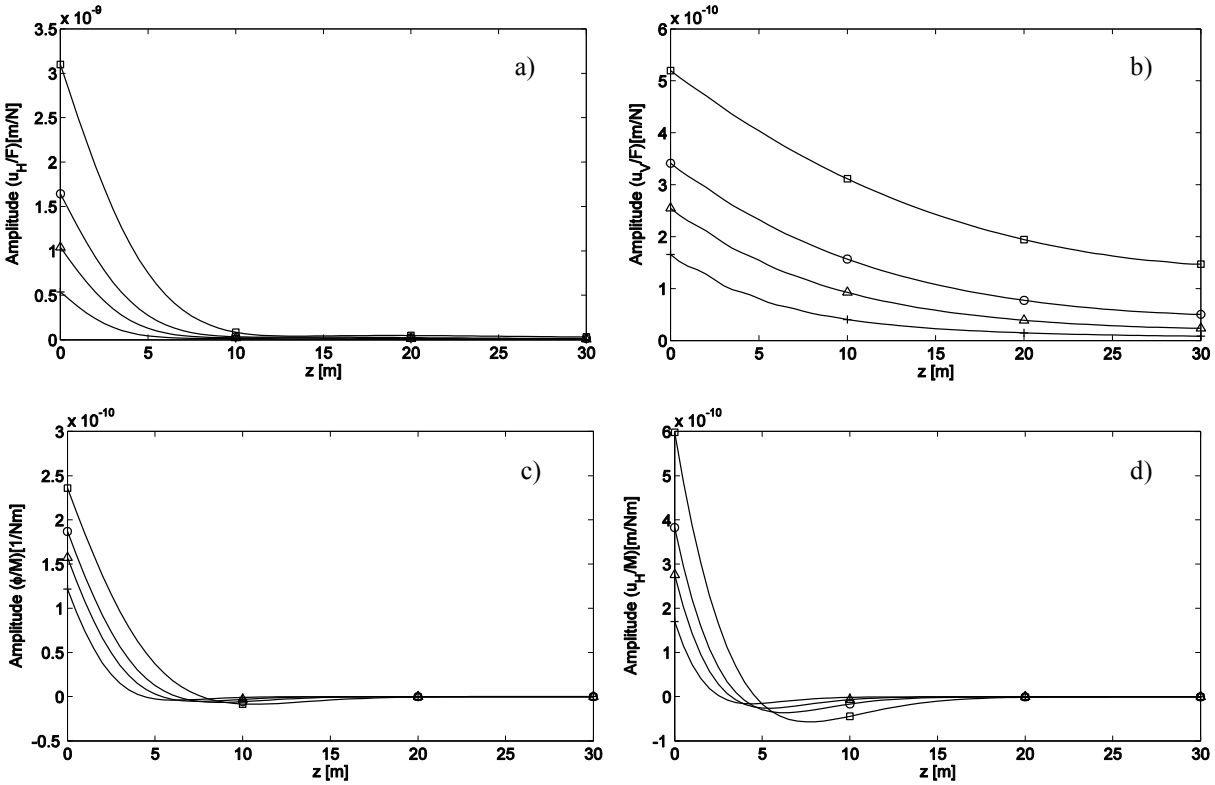

Figure 10: Static deformation of the standard pile in parabolic soil, the a) horizontal, b) vertical, c) rocking, and d) coupling component. Variation of the soil stiffness G^* = □ 2, ○ 4.5, △ 8, + 18 10^7 N/m$^{2.5}$.

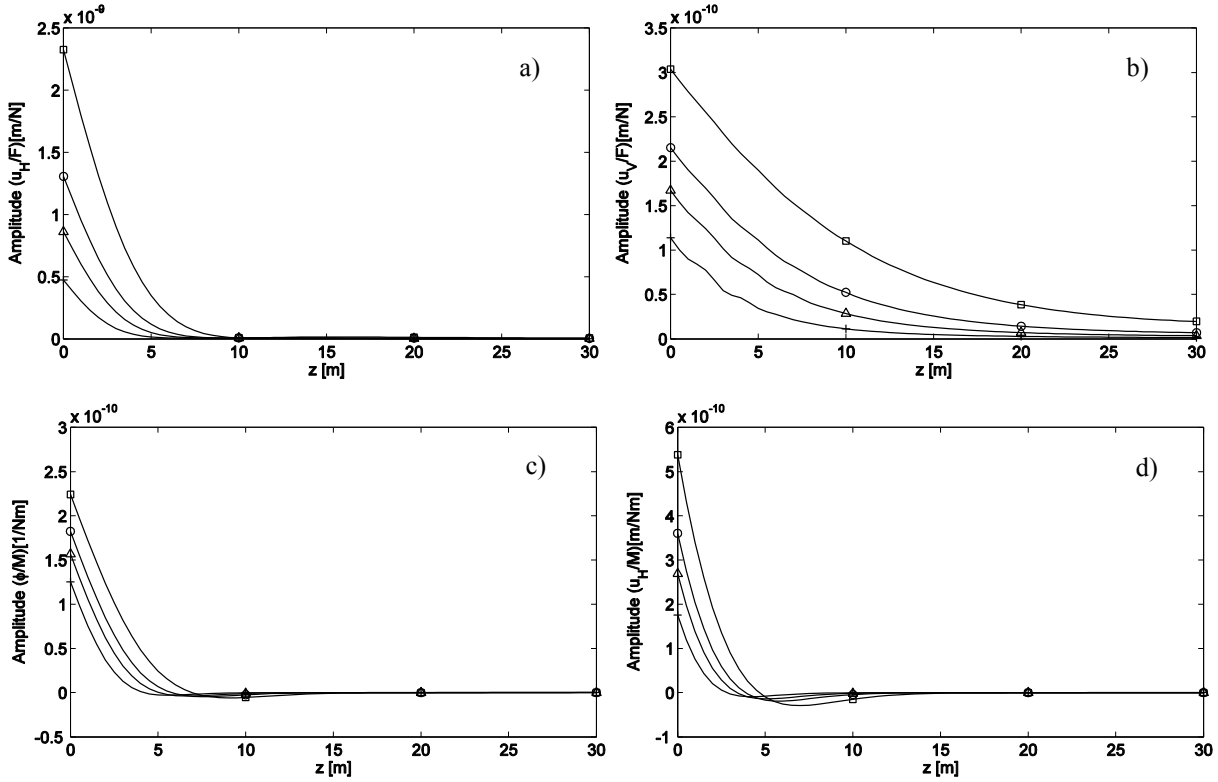

Figure 11: Static deformation of the standard pile in linearly varying soil, the a) horizontal, b) vertical, c) rocking, and d) coupling component. Variation of the soil stiffness G' = □ 2, ○ 4.5, △ 8, + 18 10^7 N/m^3.

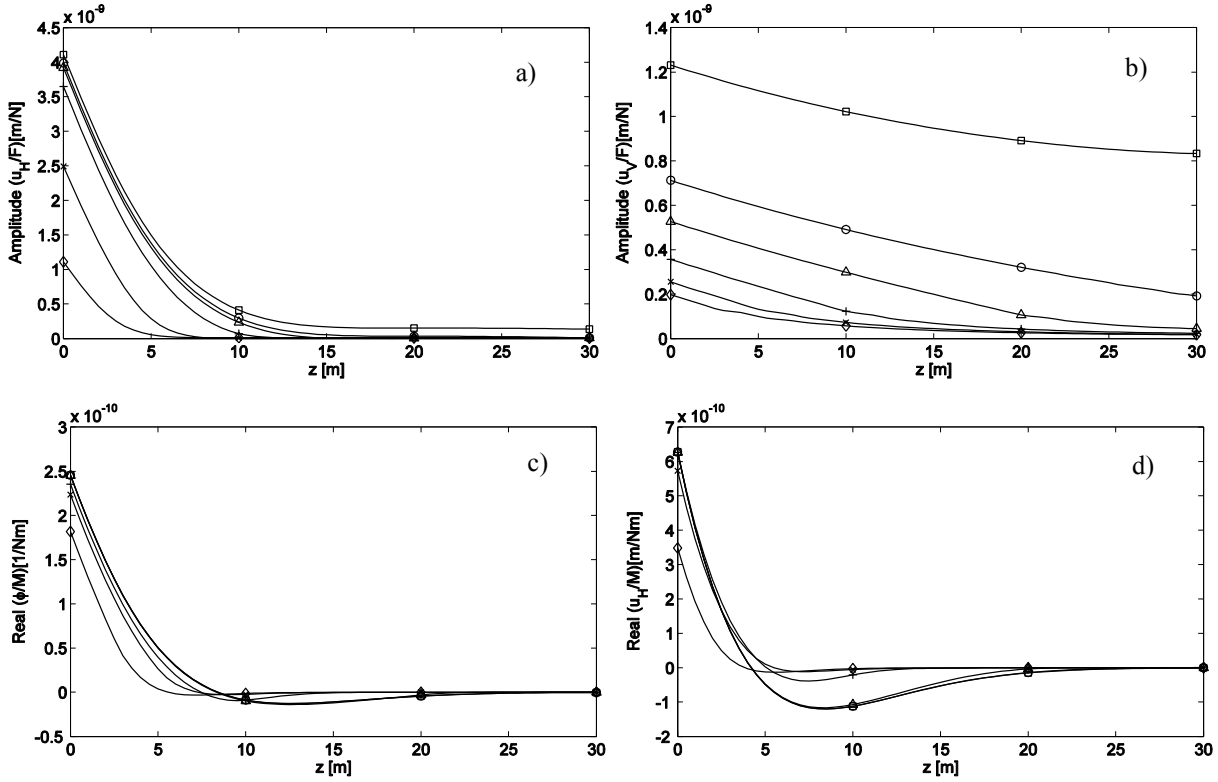

Figure 12: Static deformation of the pile in layered soils (G_1/G_2 = 2/50), the a) horizontal, b) vertical, c) rocking, and d) coupling component. Variation of the layer height H = □ ∞, ○ 30, △ 20, +10, × 5, ◇ 2.5 m.